

PAPER • OPEN ACCESS

Rock Joint Asperities and Mechanical Strength of Concrete

To cite this article: Tomáš Ficker and Tereza Komárková 2017 *IOP Conf. Ser.: Mater. Sci. Eng.* **245** 032011

View the [article online](#) for updates and enhancements.

Related content

- [Investigation into the effect of some additives on the mechanical strength, quality and thermal conductivity of clay bricks](#)
Adnan I. O. Zaid, A. Qandil and M. A. A. Qattous
- [Study on Strata Behavior Regularity of 1301 Face in Thick Bedrock of Wei - qiang Coal Mine](#)
Shuancheng Gu and Boyu Yao
- [Improvement in Durability of Piezoelectric Ceramics for Actuator](#)
Takenobu Sakai, Youichi Terai and Mamoru Ishikiriyama



IOP | ebooks™

Bringing you innovative digital publishing with leading voices to create your essential collection of books in STEM research.

Start exploring the collection - download the first chapter of every title for free.

Rock Joint Asperities and Mechanical Strength of Concrete

Tomáš Ficker¹, Tereza Komárková¹

¹ Brno University of Technology, Faculty of Civil Engineering,
Veveří 95, CZ-602 00 Brno, Czech Republic

ficker.t@fce.vutbr.cz

Abstract. Mechanical interactions between concrete foundations of large civil engineering structures (tunnels, bridges or dams) and the asperity surfaces of rock masses represent a useful topic for investigation. It is obvious that such large objects exert huge pressures on bedrocks and this might result in surprising variations of mechanical properties of the materials used in foundations. The present contribution evaluates possible changes of the compressive strength of concrete caused by the invasive acting of asperity-like needles penetrating into the volume of this material. The experimental arrangement simulates mechanical interactions between sharp asperities of bedrocks and the cement-based materials placed in the foundations of large civil engineering structures.

1. Introduction

A sufficient mechanical stability of bedrocks is the primary prerequisite for correct designs of large civil engineering structures (tunnels, bridges or dams). For assessing this stability, a lot of items are required, among others the shear strength of rock discontinuities, the degree of rock weathering, the compressive strength of intact rock, the level of ground water, the degree of infilling of rock joints, and others. If all these factors show favourable conditions, nothing from the geotechnical point of view prevents to start with building these new structures. However, there are some aspects that are usually ignored or neglected. For example, the interaction between hardened concrete and rocky surfaces, often covered by large peaked asperities, is one of these aspects that are usually considered to be unimportant. In fact, only little is known about mechanical consequences when the huge pressure of the whole structure is acting within the transition zone between the concrete foundation and the asperity surfaces of bedrocks.

In materials research there is a continuous interest in mechanical processes acting in transition zones between the hydrated cement matrix and aggregates (gravels and sand grains) [1 - 3]. However, the transition zones between concrete materials and asperity surfaces of rock joints represent rather *special zones* since the concrete material does not fully integrate asperities into its volume. The concrete only touches the asperity surface and the stability of such an interface is prevalently determined by a mechanical clasp (or wedging). Thus, the irregularity of rock surfaces is an important factor increasing the mechanical stability of concrete foundations in the slopes of rocky terrains. There are many parameters characterizing irregularity (roughness) of solid surfaces. Some of them are of a purely geometrical origin [4 - 6] but in geotechnics some special parameters were introduced that includes not only the geometrical features of surfaces but also their physical properties [7, 8].

This contribution deals with the transition zones formed by concrete materials and the asperity surfaces of bedrocks. Possible changes of the compressive strength of hardened cement-based materials



caused by the invasive acting of artificial asperity-like needles penetrating into the volume of these materials is investigated. Such an arrangement simulates mechanical interactions between sharp asperities of bedrocks and the cement-based materials placed in the foundations of large civil engineering structures.

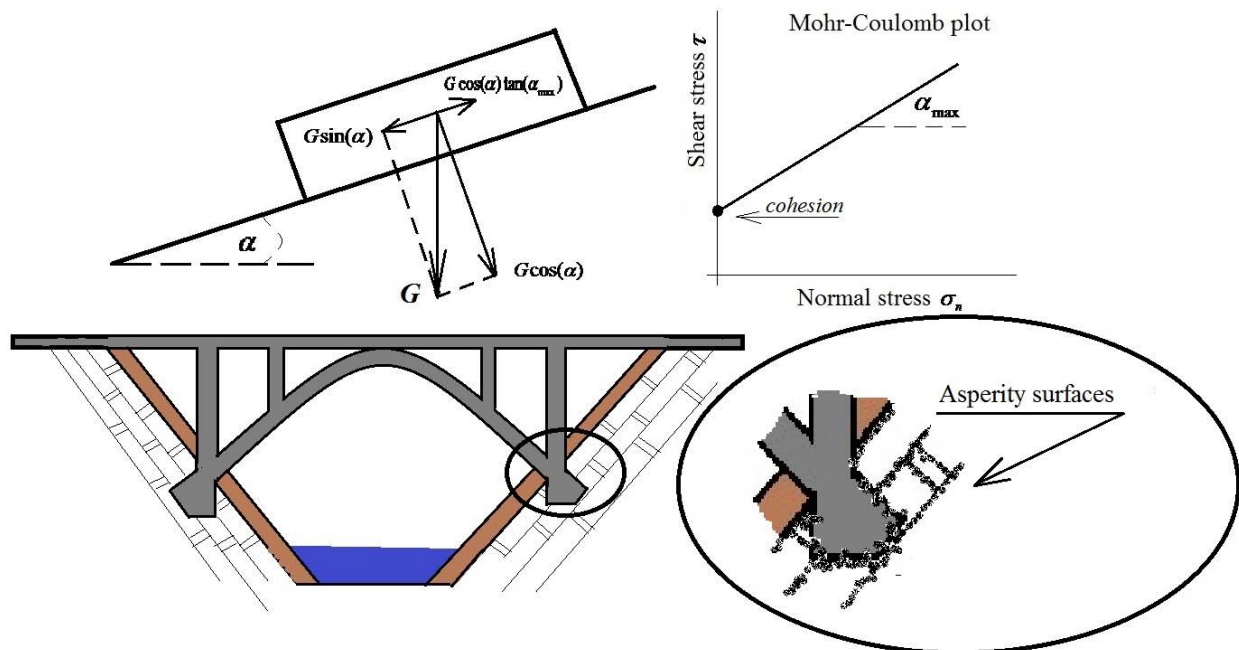


Figure 1. A scheme of rock slope stability in the terrain of rock joints

2. Rock slope stability and asperity acting

The stability of *rock joints in slopes of rocky terrains* requires the frictional forces to be equal or greater than driving forces (see figure 1)

$$G \sin(\alpha) \leq G \cos(\alpha) \tan(\alpha_{\max}) + cohesion \tag{1}$$

For assessment of the rock slope stability the factor of safety (FS) was introduced

$$FS = \frac{G \cos(\alpha) \tan(\alpha_{\max}) + cohesion}{G \sin(\alpha)} \rightarrow \left\{ \begin{array}{l} > 1 \text{ stability} \\ = 1 \text{ critical state} \\ < 1 \text{ instability} \end{array} \right.$$

(2)

If cohesion is small, then the safety factor may be expressed as follows

$$FS = \frac{\tan(\alpha_{\max})}{\tan(\alpha)} \tag{3}$$

and equation (1) simplifies as well

$$G \sin(\alpha) = G \cos(\alpha) \tan(\alpha_{\max}) \Rightarrow \tau = \sigma_n \tan(\alpha_{\max}) \tag{4}$$

where τ is shear stress and σ_n represents normal stress.

The above equations hold for perfectly smooth jointed surfaces without asperities. As soon as the asperities are present, their acting leads to better mechanical stability (wedging effects) and equation (4) has to be supplemented by an additional term i called the angle of irregularity

$$\tau = \sigma_n \tan(i + \alpha_{\max}) \quad (5)$$

Barton and Choubey [4, 5] suggested the following term for the angle of irregularity

$$i = JRC \times \log_{10} \left(\frac{JCS}{\sigma_n} \right) \quad (6)$$

where JRC is the joint roughness coefficient and JCS represents compressive strength of joint walls. At high levels of normal stresses ($\sigma_n \approx JCS$), the term $\log_{10}(JCS / \sigma_n)$ approaches zero, which means that asperities are sheared off from the surface of joint walls and the irregularity angle i fully diminishes. Barton and Choubey in accordance with equation (5) obtained the following expression for the *shear strength of rock joints* [7, 8]

$$\tau = \sigma_n \tan \left[JRC \cdot \log_{10} \left(\frac{JCS}{\sigma_n} \right) + \alpha_{\max} \right] \quad (7)$$

The overall mechanical stability of foundations depends both on the stability of bedrock (see shear strength specified by equation (7) or the scheme in figure 1) and the stability of the transition zones between concrete and asperity surfaces of bedrocks. The shear strength of bedrocks has been briefly discussed in the foregoing paragraphs and the stability of the transition zone will be discussed in the next sections.

The mechanical stability of the transition zones between the asperity surfaces of bedrocks and the concrete material will be investigated experimentally by means of the arrangement in which the role of sharp asperities will play the metallic needles shown in figure 2. *The invasive acting of the needles when subjected to compressive load will be tested and the changes of compressive strength of concrete will be studied. The aim of these tests is to find the dependence of compressive strength of concrete on the length of the needles.*

3. Experimental arrangement

To simulate acting of sharp needles on the compressive strength of plain concrete, a series of specimens containing steel needles of various lengths were prepared. The concrete material was mixed from sand with grains 0.1 - 0.4 mm and cement Cemi I 42,5 R produced in the Czech Republic. The water-to-cement-to-sand ratio was 1:1.943:7.773 by weight, i.e. the water-to-cement ratio was 0.515 by weight. 48 specimens (10cm x 10cm x 10cm) were moulded at normal laboratory conditions. They were divided into 8 groups each of them contained 6 specimens. Seven groups contained specimens with imbedded steel needles of different lengths (5 mm, 7 mm, 11 mm, 19 mm, 29 mm, 40 mm and 58 mm) while the eighth group consisted of *needleless* specimens. After 28 days of hydration in water (20°C) the specimens were subjected to compressive tests and resulted values were averaged within each group of specimens. Three specimens that experienced the final destructive tests can be seen in figure 2 along with the steel needles.



Figure 2. Concrete specimens containing steel needles after the final destructive tests.

4. Results and discussions

The averaged values of compressive strength of eight investigated groups can be seen in figure 3. The values of compressive strength have been plotted against the relative lengths of the steel needles ρ

$$\rho = \frac{h}{H} \times 100 (\%), \quad H = 100 \text{ mm} \quad (8)$$

where h and H are heights of the needles and the concrete specimens, respectively.

The graph in figure 3 illustrates an unusual behaviour of compressive strength of concrete specimens. The specimens with short needles ($\rho < 10\%$) show increasing compressive strength whereas the compressive strength of the specimens with larger needles ($\rho > 10\%$) decreases. The decrease is at first very rapid ($\rho \in (10\%, 20\%)$) but for quite large needles $\rho > 20\%$ the decrease of compressive strength is considerably reduced.

The behaviour of compressive strength may be characterized by two critical points. The first of them represents a critical needle length at which the specimens show the highest value of strength, i.e.

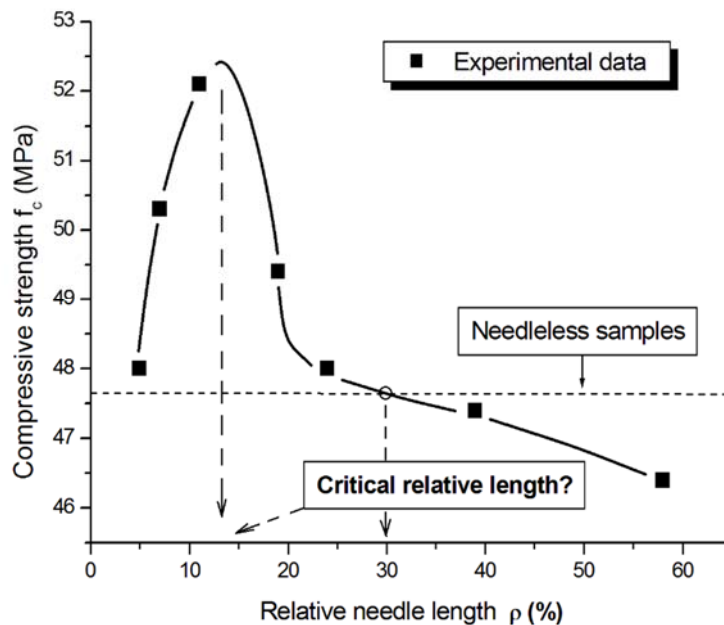


Figure 3. Compressive strength of concrete specimens containing steel needles

$\rho_1 \approx 10\% - 15\%$. The second critical point $\rho_2 \approx 30\%$ is specified by the crossing of the graph of compressive strength with the horizontal dashed line which represents the compressive strength of the *needleless specimens*. Left to the second critical point there are specimens showing higher strength whereas right to it the specimens show lower strength as *compared with the normal needleless specimens*.

It is not a straightforward matter to find a thorough and reliable explanation for such an exceptional behaviour of compressive strength. Certainly, it is the needle length that play a crucial role. The short needles strengthen the concrete cubes whereas the longer needles reduce compressive strength. Probably, the shorter needles do not represent large perturbations in the cube structure and act as a certain type of reinforcement in the lower parts of these cubes. On the other hand, the longer needles may represent larger perturbations in concrete specimens and as such they may weaken the structure rather than reinforce it.

If these ideas are sound, then the data related to the decreasing sequence of the graph in figure 3, i.e. the data right to the first critical point ($\rho > \rho_1$), should approach some type of the known functional patterns for defective behaviours. For example, one of the widely known functional patterns of this kind quantifies a destructive structural influence of pores in solid structures and usually is written as an exponential function correlating porosity P and compressive strength f_c

$$f_c = f_o \exp(-kP) \quad (9)$$

where f_o is compressive strength of non-perturbed structure and k is a fitting constant. Pattern (9) is applicable to variety of materials including iron, plaster of Paris, sintered alumina, and, of course, cement-based materials. This pattern holds for many solid materials and as such it may be considered as a general relation quantifying defective influences of various structural perturbations P .

All our specimens had approximately the same porosity since they were prepared with the same water-to-cement-to-sand ratio and were treated and stored under the same laboratory conditions. However, when accepting the idea that P may represent not only porosity but also another type of structural perturbations, we may introduce a new concept of defective acting and modify accordingly the interpretation of P .

In the present experiments, the role of structural perturbations play the steel needles of *longer relative lengths* $\rho > \rho_1$. By expressing their *volume* v relative to the total *volume* of the concrete cube V analogously as in the case of porosity, a new classifying factor emerges that might be called the *metallicity*¹⁾ of concrete M

$$M = \frac{v}{V_o} \times 100 (\%), \quad v = n \cdot h \cdot \pi \cdot r^2, \quad V_o = H^3 = 1000 \text{ cm}^3 \quad (10)$$

where $n = 30$ is the number of needles in one concrete cube and $r = 2 \text{ mm}$ is the radius of the used needles. By replacing porosity P by concrete metallicity M in equation (9) a new pattern for investigation of the defective acting of longer steel needles $\rho > \rho_1$ emerges

$$f_c = f_o \exp(-kM), \quad \rho > \rho_1 \quad (11)$$

In this study a slightly modified pattern has been used

$$f_c = f_o \exp(-kM) + f_1, \quad \rho > \rho_1 \quad (12)$$

The reason is that M in contrast to P is restricted in its extent. For example, f_c in equations (11)/(12) cannot approach a real value f_o of the needleless cubes since these patterns describes only the region right to the first critical point $\rho > \rho_1$ and for the left interval $\rho < \rho_1$ the patterns are inapplicable. In addition, M cannot go to "infinity" since the length of the needles are restricted by the size of the cubes H . Thus the maximum value of M is restricted by the maximum length of the needles ($h_{\max} = H$) and their numbers n (in our case $n = 30$). Thus, for maximum M_{\max} the following relation has to be fulfilled

$$f_c(M_{\max}) \approx \lim_{M \rightarrow \infty} f_c(M) = f_1 \quad (13)$$

In order to test the functionality of pattern (12), it has been fitted by using the least square method to the measured data that correspond to longer needles $\rho > \rho_1$. The following optimized coefficients have been received: $f_o = 12.843 \text{ MPa}$, $f_1 = 46.403 \text{ MPa}$, $k = 2.022$. The resulted graph can be seen in figure 4. Obviously, the fitting pattern (12) closely follows the experimental data with high correlation coefficient 0.990 which supports soundness of the concept of metallicity of concrete. For completeness, the criterion (13) may be verified. The maximum value of concrete metallicity amounts to 3.77 %. Inserting this value in equation (12), the resulted value of compressive strength is received $f_c(M_{\max}) = 46.409 \text{ MPa}$, which corresponds almost exactly to the optimized value $f_1 = 46.403 \text{ MPa}$.

¹⁾ In astronomy, the *metallicity* of an astronomical object is defined as the ratio of the mass of elements heavier than hydrogen and helium to the *total mass* of hydrogen and helium that are present in the object.

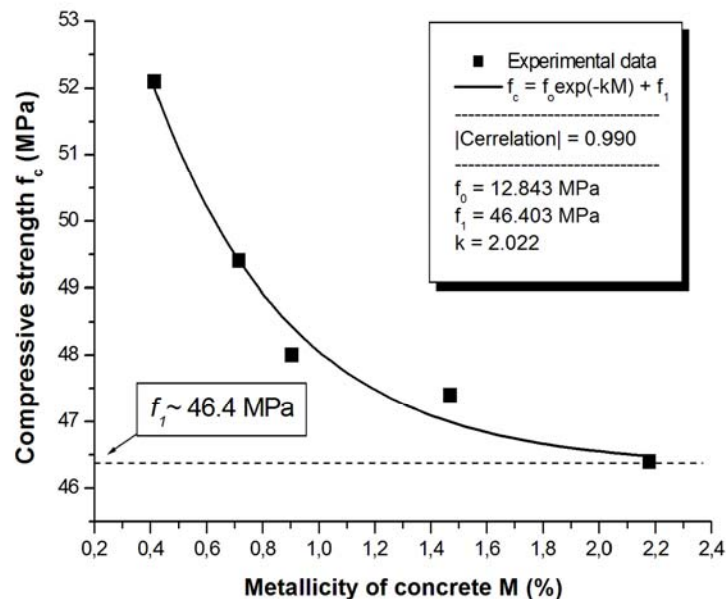


Figure 4. Compressive strength of concrete influenced by longer steel needles $\rho > \rho_1$

5. Conclusions

This study has revealed a positive influence of *short needles* on the compressive strength of plain concrete. However, negative acting of *longer needles* on the mechanical integrity of concrete has resulted in lower values of compressive strength. These results might be applied to the transition zones between the asperity protrusions of bedrocks and concrete in foundations of civil-engineering constructions. Since the several centimetres high asperities can be considered as quite short needles in comparison with the common height of concrete foundations, it is likely that the acting of such short protrusions may have a positive influence on the concrete integrity rather than negative impacts. The necessary prerequisite of such an assumption is that the compressive strength of the rock material is larger than the compressive strength of concrete. This is especially fulfilled with high quality rock materials such as granite, basalt, gneiss and others.

Acknowledgment(s)

This paper has been supported by the Grant Agency of the Czech Republic under grant No. 13-03403S. Thanks are also due to Mr. Pavel Kropáček for technical support.

References

- [1] Mielniczuk, B., Jebli, M., Jamin, F., El Youssoufi, M. S., Pelissou, C., Monerie, Y., 2016. Characterization of behavior and cracking of a cement paste confined between spherical aggregate particles. *Cement and Concrete Research*, 79: 235-242 (DOI: 10.1016/j.cemconres.2015.09.016).
- [2] Wu, K., Shi, H. S., Xu, L. L., Ye, G., De Schutter, G., 2016. Microstructural characteriyation of ITZ in blended cement concretes and its relation to transport properties. *Cement and Concrete Research* 79: 243-256 (DOI: 10.1016/j.cemconres.2015.09.018).
- [3] Wang, X.H., Jacobsen, S., He, J.Y., Zhang, Z.L., Lee, S.F., Lein, H.L., 2009. Application of nanoindentation testing to study of the interfacial transition zone in steel fiber reinforced mortar. *Cement and Concrete Research*, 39 (8): 701-715 (DOI: 10.1016/j.cemconres.2009.05.002).

- [4] Ficker, T., Martišek, D., 2011. Roughness and fractality of fracture surfaces as indicators of mechanical quantities of porous solids. *Central. Europ. J. Phys.*, 9: 1440-1445.
- [5] Ficker, T., Martišek, D., Jennings, H. M., 2011. Surface roughness and porosity of hydrated cement pastes. *Acta Polytechnica* 51: 7-20.
- [6] Ficker, T., 2012. Fracture surfaces and compressive strength of hydrated cement pastes. *Constr. Build. Mater.*, 27: 197-205.
- [7] Barton, N., 1973. Review of a new shear-strength criterion of rock joints. *Engineering Geology*, 7 (4): 287-332.
- [8] Barton, N., Choubey, V., 1977. The shear strength of rock joints in theory and practice. *Rock. Mech.*, 10 (1): 1-65.
- [9] Mehta, P. K., Monteiro, P. J. M., 2006. *Concrete, Microstructure, Properties and Materials*, 3rd edn. McGraw/Hill, New York (page 50).